



Mathematical Modelling of "Asd Tug - Marine Vessel" Interaction Considering Tug's Maneuverability and Stability Limitations

Oleksandr Pipchenko^{1,*}, Nataliia Konon², Yevgen Bogachenko³

ARTICLE INFO

Article history:

Received 7 Apr 2023;
in revised from 28 Apr 2023;
accepted 29 Jun 2023.

Keywords:

safety of navigation, mathematical modelling, simulations, vessel motions, vessel-tug interaction, ASD tug, manoeuvrability.

© SEECMAR | All rights reserved

ABSTRACT

The research addresses the problem of vessel-tug operation in context of tugboats' manoeuvrability and stability limitations, which are often overlooked. Proposed mathematical model of Azimuth Stern Drive tug's dynamics considers the stability features and is used for the simulation of vessel-tug system's dynamics in the "bow-to-bow", "stern-to-bow" and "girting" modes. Based on the results of emergency situations' modelling concerning a tugboat working on a towline, critical values were identified for the difference between the tug's and the vessel's headings, as well as the speed ratio, leading to the emergency state of the tugboat. The list of such conditions is presented in the article and may be used as recommendations when planning and monitoring the vessel-tug system's operation.

1. Introduction.

Nowadays, the positive trend in the economic and environmental efficiency of maritime transport is constantly required by the nature of globalization, which implies an increase in the volume of cargo to be transported at relatively reduced shipping costs. This can be achieved by increasing the carrying capacity of ships. For example, in May 2022, m/v "EVER ALOT" - a new ULCS with a capacity of 24,004 TEU was launched, the first of the six largest container ships planned to be launched by Evergreen. The standard dimensions of this type of vessels are about 400 m in length, 62 m in width and a maximum draft up to 17 m. Thus, with a fully loaded deck, the sail area may reach up to 9 thousand square meters, which, consequently, may have a significant impact on manoeuvrability at specific relative wind speed. Statistical data on maritime accidents on container ships, indicating the primary and secondary causes of the cases studied, were discussed in [10].

Over the past 10 years, maritime trade has mostly shown a positive trend, with rates ranging from 0.5 to 4.8%, according to UNCTAD review of maritime transport [31]. However, in 2020, due to the COVID-19 pandemic, maritime trade decreased by 3.8%. In 2021, by contrast, global merchandise trade increased by 4.3%, which has resulted in additional port congestion and reduced levels of service and reliability.

From a manoeuvring point of view, the most critical stages of navigation are associated with congested areas, such as rivers, harbours, canals, etc., where pilotage and towing services are compulsory and provided by local regulations. According to EMSA statistics for the period from 2014 to 2020, 55% of maritime accidents occurred in inland waters, especially in port areas. Among service vessels, 26% of casualties involved tug vessels, while more than half of the accidents (58.4%) were related to the navigational nature, i.e., contact, grounding, stranding, capsizing, and collision involving multi-vessel operation. Based on the analysis conducted during the investigations, it was stated that during the same period, 89.5% of incidents had been related to human erroneous actions [5].

Controllability and stability of tug vessels during the operations with a towed object are critical characteristics that shall be considered in conjunction with the escort or towing operations

¹National University "Odesa Maritime Academy".

²National University "Odesa Maritime Academy".

³National University "Odesa Maritime Academy".

*Corresponding author: Oleksandr Pipchenko. E-mail Address: nav.researches@gmail.com.

objectives. Therefore, this research is focused on the problem of vessel-tug interaction simulation and the feasibility of existing technical solutions' implementation to improve the safety of navigation.

2. Literature review and problem statement.

In general, based on purpose, tugs are classified into two main groups: escort tugs and support tugs. Escort tugs designed to escort and manoeuvre vessels to their destination, while support tugs are used to provide support services for offshore and towing operations. Based on the design, marine industry tugs are mainly of three types: conventional tug, tractor tug and Azimuth stern drive (ASD) tug.

In this article, the mathematical modelling of the tug's motion is focused on the ASD escort tugs, which are equipped with azimuth thrusters and allow safe operations at speeds of 4-8 knots [22].

The significant advantages of ASD tugs include such features as better directional stability at speed, hull form designed for open waters and seaway, improved bollard pull, average draft of 3m etc.

ASD tugs are widely studied in terms of modelling and evaluating their manoeuvrability and efficiency in various modes, in particular to simplify the acquisition of experimental data for shipbuilding purposes. For example, braking force was evaluated in [33] when interacting with VLCC in astern and ahead thrust methods. An advanced equilibrium resolution methods were proposed in [14] considering each propulsive device of ASD tug as an independent actuator. The behaviour of a steerable thruster was simulated by means of a 4-quadrant modelling of a ducted propeller, taking into account cross-flow effect. The results of calculations performed on the reference tug showed that proposed method predicts a wider range of acceptable equilibrium solutions compared to the simplified procedures and/or their extended versions such as the iterative method.

Within the scope of defining a parametric manoeuvring simulation code for the free-sailing and towing operations for ASD tug an extensive research has been carried out [17-21]. Experimental Fluid Dynamics (EFD) method was used to develop and validate the manoeuvrability code based on the performances measured onto reference tug. With an extensive analysis of the 4-DoF PMM results, the hydrodynamic forces acting onto prototype tug were modelled and validated in [17], covering the degrees of freedom of the tug in the horizontal plane and the heel angle. Computational Fluid Dynamics (CFD) simulations were performed to test and validate numerical procedures to evaluate hydrodynamic forces onto the original prototype. At the next stage EFD and CFD manoeuvring models were examined and validated in [18], while research [19] is focused on the hydrodynamic characterization of a series of skeg designs. A physics-based 4-DOF prediction parametric tool for the dynamic behaviour of the ASD tug, as well as a validation with model-scale escort-towing tests were presented in [20]. In further work a second validation methodology was discussed, based on full-scale measurements, showing a satisfactory agreement with the full scale manoeuvres, positively

demonstrating the ability of the parametric mathematical formulations to forecast customised tug manoeuvrability for tug design purposes [21].

Following studies [1-3, 9, 15, 16, 26, 24, 35] provide the mathematical model structure of the tugboat with the reflection of general forces acting on it. However, more detailed data, such as calculation functions for individual forces and coefficients, is not reflected in the mentioned studies.

In general, mathematical models of tugboat dynamics can be divided into two main groups: movement on the plane [1, 7] and movement on the plane with an account for stability [2, 3].

3. Materials and Methods .

3.1. Critical factors of tugboat stability.

Nowadays, stability requirements for tugs are not agreed upon the international level, in particular those established for tugs of a smaller size. Some of the requirements do not take into consideration abnormal forces on the towing line. Although classification society or flag state may regulate minimum stability information to be provided, which does not guarantee that abnormal towline forces would be considered.

The heeling moment occurring during towing, together with the applied safety margin determines the stability of a tug. When towing, the heeling moment can be produced by:

1. The tow – tow tripping, when the tug is dragged by the tow, via the towline at a certain speed and a certain course through the water.
2. The tug – self-tripping, when the heeling moment is caused by the combined action of rudders, propellers and the towline force or hydrodynamic lateral force on the hull; decisive are the thrust forces or bollard pull of the tug.
3. A combination of tow and tug.

In general, the following accidents may occur during towing [24]:

- girting;
- collision or contact with the fixed object or installation;
- parting of a towline;
- grounding of the tug or tow;
- main propulsion power or electrical power loss;
- steering failure;
- critical control systems failure etc.

Girting, girding, or tripping (GGT) define the situation when the tug is towed broadside by a towline and therefore unable to manoeuvre. This is a common cause of tug capsizing and can lead to loss of life [27]. Instant release of the towline is essential to avert distress, as such a situation develops quickly and can occur at either end of the tugboat. Despite the safety instructions during tug crew training, according to marine investigation reports the girting phenomenon continues to be a concern [11-13, 28-30].

3.2. Tugboat motion equations.

The system of equations that describes the tug’s motion in general form is defined as:

$$\begin{aligned} (m + m_{11})\dot{u} - (m + m_{22})vr &= X \\ (m + m_{22})\dot{v} + (m + m_{11})ur &= Y \\ (I_{44} + J_{44})\dot{p} &= K \\ (I_{66} + J_{66})\dot{r} &= N - x_G Y \end{aligned} \quad (1)$$

where:

m is the displacement of the vessel;

m_{11}, m_{22} – added masses;

I_{44}, I_{66} – moments of inertia;

J_{44}, J_{66} – added moments of inertia;

u, v, p, r – longitudinal and transverse components of translational velocity and angular velocities relative to the transverse and vertical axes relative to the centre of gravity (x_G) of the vessel respectively;

X, Y, K, N are hydrodynamic forces and moments acting on the vessel.

In an expanded form, hydrodynamic forces and moments are presented as follows:

$$\begin{aligned} X &= X_H + X_P + X_{\gamma L} \\ Y &= Y_H + Y_P + Y_{TL} \\ K &= K_H + K_P + K_{TL} + K_{ROLL} \\ N &= N_H + N_P + N_{TL} \end{aligned} \quad (2)$$

where:

H – hull;

P is propeller-stern group generalized force;

TL – towing line tension;

R – restoring moment and inertia.

The resistance forces on the body are defined as:

$$\begin{aligned} X_H &= \frac{1}{2}C_{HX}(u, \beta, r) \cdot \rho L d U^2 \\ Y_H &= \frac{1}{2}C_{HY}(\beta, r) \cdot \rho L d U^2 \\ K_H &= (z_H - z_G) \cdot Y_H \\ N_H &= \frac{1}{2}C_{HN}(\beta, r) \cdot \rho L^2 d U^2 \end{aligned} \quad (3)$$

where:

C_H - the coefficients of forces and moments of resistance along the respective axes;

ρ is seawater density;

L is the vessel’s length;

d is the vessel’s draft;

U is the absolute speed of the vessel;

u is the longitudinal component of the vessel’s speed;

β is the drift angle (positive and counter clockwise);

r is the rate of course change;

z_G is the centre of gravity along Z-axis;

z_H is the centre of the submerged part of the hull along Z-axis.

Normally, C_H coefficients can be obtained in experimental way [1, 3, 15], although these coefficients can also be approximately determined using the methods presented in [7, 32, 34].

3.3. Forces produced by azimuth thrusters.

The force generated by the thrusters is defined as a total value $F_P > 0$, according to [1]. However, the direction of the application of F_P depends on the set rotation angle δ . Such a condition is valid for the synchronous operation of azimuth thrusters in stable towing modes. For the operations with azimuth thrusters, a common way to reduce speed or tension and change the load is to rotate propeller pods to the sides at angles from 30 to 150 degrees, depending on the direction of movement. One more method is called "asynchronous" control, which involves one propeller working in longitudinal direction only, and the other performing rotation. Thus, in order to properly simulate the towing manoeuvre, the pod groups have to be considered separately.

The thrust of the single propeller is determined as:

$$F_P = (1 - t)\rho \cdot K_T(J, \theta_P) D_P^4 n |n| \quad (4)$$

$$J = |U_P(1 - w)/nD_P| \quad (5)$$

where:

t – empirical coefficient of the thrust reduction;

n – propeller revolutions;

D_P – diameter of the propeller;

K_T – thrust factor;

J – propeller slip;

θ_P – rotation angle of the propeller blades;

U_P – flow velocity on the propeller;

w – empirical hull influence factor.

In equation (4) the revolutions are presented as $n|n|$ to simulate the reverse operation of the propeller, instead of the standard accepted form n^2 .

Interaction effects have to be considered when both propellers push towards the same direction. Methods describing the consideration of propellers interaction can be found in research [3, 4]. Effective thrust on the propeller located in front is decreased by the flow thrown onto it by the propeller from behind [1]. Sufficiently accurate method for approximate modelling is defined as [4]:

$$F_P^* = C_{t\theta} F_P \quad (6)$$

$$C_{t\theta} = C_t + (1 - C_t) (\theta^3 / 130 / C_t^3 + \theta^3) \quad (7)$$

$$C_t = 1 - 0,8(l_P / D_P)^{2/3} \quad (8)$$

where:

$C_{t\theta}$ – interaction coefficient;

θ – the angle between axes of azimuth thrusters;

C_t – interaction coefficient at $\theta = 0$;

l_P – the distance between propellers.

Forces on the port and starboard thrusters are defined as [22]:

$$\begin{aligned} X_P &= F_P^S \cos \delta_S + F_P^P \cos \delta_P \\ Y_P &= F_P^S \sin \delta_S + F_P^P \sin \delta_P \\ K_P &= (z_P - z_G) \cdot Y_P \\ N_P &= x_P \cdot Y_P - y_P^S \cdot F_P^S \cos \delta_S - y_P^P \cdot F_P^P \cos \delta_P \end{aligned} \quad (9)$$

where:

F_P – propeller thrust;

δ - thruster angle;

x_P, y_P, z_P – coordinates of the respective thruster.

In this case, the lateral force component created by the propeller rotation is not taken into consideration.

3.4. Tugboat stability consideration.

The equation of roll oscillations [6]:

$$a_{42} \cdot \dot{v}_G + b_{42} \cdot v_G + (I_{kk} + a_{44}) \dot{p}_G + b_{44} \cdot p_G + a_{46} \cdot \dot{r}_G + b_{46} \cdot r_G = K \quad (10)$$

where:

a – inertia forces coefficients;

b – damping forces coefficients;

K – heeling moment;

φ – roll angle;

indices 1, 2, 3 correspond to linear movements along the longitudinal, transverse, and vertical axes;

indices 4, 5, 6 correspond to rotation relative to the longitudinal (roll), transverse (pitch) and vertical (yaw) axes of the vessel.

The rolling of the ship during the manoeuvre does not have a periodic character, contrary to the roll of the vessel in the waves. Coefficients of the damping forces at the theoretical wave frequency close to zero are absent, except for coefficient b_{46} , which depends on the added masses, and the coefficient b_{44v} , which expresses nonlinear viscous damping [8]. Considering the transformations due to zero theoretical wave frequency equals, coefficients a_{42} , a_{44} , a_{46} , b_{46} are determined as follows:

$$\begin{aligned} a_{42} &= m_{42} + OG \cdot m_{22} \\ a_{44} &= m_{44} + m_{42} + OG \cdot (m_{24} + OG \cdot m_{22}) \\ a_{46} &= (m_{42} + OG \cdot m_{22}) \cdot L \\ b_{46} &= -u \cdot (m_{42} + OG \cdot m_{22}) \end{aligned} \quad (11)$$

where:

m_{ii} – added masses' coefficients;

OG – the length of the perpendicular lowered from the centre of gravity to the plane of the waterline;

L – length of the vessel between perpendiculars;

u - forward speed of the ship.

Using Ikeda's method [6], coefficient b_{44v} can be determined, excluding the components dependent on the theoretical wave frequency:

$$b_{44v} = b_{44f}(\varphi_a, \omega_n, u) + b_{44l}(u) \quad (12)$$

where:

b_{44f} –friction coefficient;

b_{44l} – lift coefficient;

φ_a – heel angle amplitude;

ω_n – frequency of the oscillations.

As a result, the roll moment K_R is calculated as follows:

$$K_R = a_{42} \cdot \dot{v}_G - a_{46} \cdot \dot{r}_G - b_{46} \cdot r_G - b_{44v} \cdot p_G - K_\varphi \quad (13)$$

where K_φ - restoring moment.

In case of the lack of detailed information on stability, the restoring moment can be calculated as:

$$K_\varphi = g \cdot m \cdot l(\varphi) \quad (14)$$

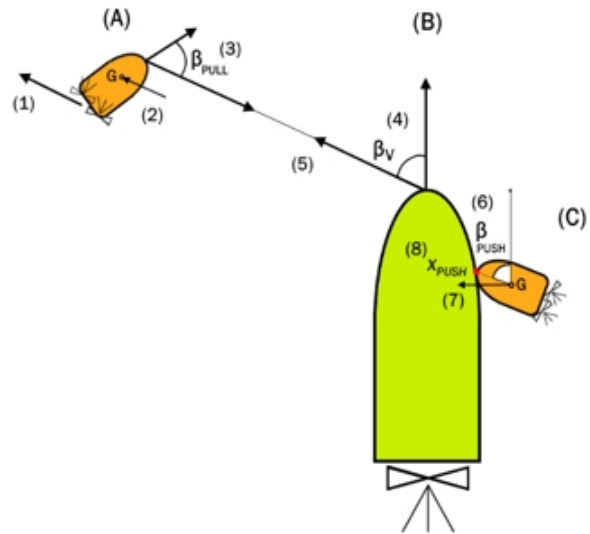
where $l(\varphi)$ – the roll-dependent arm of static stability.

3.5. Towline tension consideration.

A simplified diagram of the vessel and tugs (pushing and pulling) interaction is shown in Figure 1. Mathematical model of the towline tension presented in this work does not consider the elasticity of the towline. The calculation of the line tension begins after reaching the specified length l_{TL} . Tension F_T equals zero in case the distance between the connection points of the towline on ships is less than l_{TL} .

In Figure: (A) Pull mode; (1) Total thrust force ($F_P > 0$); (2) Generalized vector of hydrodynamic forces: hull + inertia ($F_H + F_I$); (3) β_{PULL} – towline angle (drift angle of tug hull); (B) Towed vessel; (4) β_V – drift angle of the vessel's hull; (5) Towline tension ($F_{PULL} > 0$); (C) Push mode; (6) β_{PUSH} – push angle (drift angle of tug hull); (7) Generalized vector of push forces: hull + push force + push reaction force ($F_H + F_P + F_R$); (8) x_{PUSH} – point of pushing on vessel.

Figure 1: Simplified diagram of the vessel-tug interaction.



Source: Authors

To transfer the force of the tug to the stretched towline, the resulting force R created by the tug should be non-zero and act in the direction away from the towed object.

$$\begin{aligned} F_{PULL X} &= 0 \text{ if} \\ R_X &< 0 \wedge \beta_{PULL} \in \left(-\frac{\pi}{2}; \frac{\pi}{2}\right), \text{ when } x_T < 0 \\ R_X &> 0 \wedge (\beta_{PULL} > \frac{\pi}{2} \vee \beta_{PULL} < -\frac{\pi}{2}), \text{ when } x_T \geq 0 \end{aligned} \quad (15)$$

$$\begin{aligned}
 &F_{PULL Y} = 0 \text{ if} \\
 &\&R_Y > 0 \wedge \beta_{PULL} \in (0; \pi) \\
 &\&R_Y < 0 \wedge \beta_{PULL} \in (-\pi; 0)
 \end{aligned} \quad (16)$$

where $F_{PULL X}$, $F_{PULL Y}$ – longitudinal and transverse components of pulling force; R_X , R_Y – longitudinal and transverse components of the equivalent R; β_{PULL} – towline angle, x_T – coordinate of towline fix point.

The longitudinal and transverse components of the equivalent R are transmitted to the towline along its direction, creating tension F_T :

$$F_{PULL X} = R_X \cdot \cos\beta_{PULL}; F_{PULL Y} = R_Y \cdot \sin\beta_{PULL} \quad (17)$$

$$F_{PULL} = F_{PULL X} + F_{PULL Y} + F_{PULL V} \quad (18)$$

where $F_{PULL V}$ – additional tension from the towed vessel. In this case, reacting forces can be defined as follows:

$$\begin{aligned}
 X_{PULL} &= F_{PULL} \cdot \cos\beta_{PULL} \\
 Y_{PULL} &= F_{PULL} \cdot \sin\beta_{PULL} \\
 N_{PULL} &= Y_{PULL} \cdot x_{PULL} \\
 K_{PULL} &= Y_{PULL} \cdot (z_{PULL} - z_G)
 \end{aligned} \quad (19)$$

When the tugboat reaches the length of the towline an impulse force occurs. As a result, tugboat and the towed object velocities become equal. To avoid theoretical “stretching” of the rope in calculations, a kinematic condition was introduced: if the rate of the rope extension is positive when the maximum length is reached, it is subtracted from the tug’s speed along the corresponding axes.

$$\begin{aligned}
 &l_{TP} > l_{TL} - \frac{dl_{TP}}{dt} \\
 &u' = u - \frac{dl_{TP}}{dt} \cos\beta_{PULL} \\
 &v' = v + \frac{dl_{TP}}{dt} \sin\beta_{PULL}
 \end{aligned} \quad (20)$$

For the system, where several tugboats are pulling the vessel, the equation (19) will take following form to describe the resultant force:

$$\begin{aligned}
 X_{PULL N} &= \sum_{n=1}^N F_{PULL n} \cdot \cos\beta_{PULL n} \\
 Y_{PULL N} &= \sum_{n=1}^N F_{PULL n} \cdot \sin\beta_{PULL n} \\
 N_{PULL N} &= \sum_{n=1}^N Y_{PULL n} \cdot x_{Tn} \\
 K_{PULL N} &= \sum_{n=1}^N Y_{PULL n} \cdot (z_{PULL n} - z_G)
 \end{aligned} \quad (21)$$

where N – total number of tugs involved in pulling, n – tug number (from 1 to N).

3.6. Consideration of tug pushing force.

The calculation of the pushing force begins from the moment the tug reaches the kinematic boundary – the ship’s hull. To transfer the pushing force of the tug to the hull of the object, the resulting force created by the tug has to be positive, act in the direction of the towed object and the distance between the hulls of the tug and the object must be equal to zero: $x_{PUSH} = 0$. During simulation modelling in Matlab R2016a, the function “inpolygon” was used to determine the moment of contact between the tug hull and the ship hull.

$$\begin{aligned}
 &F_{PUSH X} = 0 \text{ if} \\
 &R_X < 0 \wedge \beta_{PUSH} \in \left(-\frac{\pi}{2}; \frac{\pi}{2}\right), \text{ when } x_{PUSH} = 0 \\
 &R_X > 0 \wedge \beta_{PUSH} \in \left(-\frac{\pi}{2}; \frac{\pi}{2}\right), \text{ when } x_{PUSH} > 0
 \end{aligned} \quad (22)$$

$$\begin{aligned}
 &F_{PUSH Y} = 0 \text{ if} \\
 &R_Y > 0 \wedge \beta_{PUSH} \in (0; \pi) \\
 &R_Y < 0 \wedge \beta_{PUSH} \in (-\pi; 0)
 \end{aligned} \quad (23)$$

where $F_{PUSH X}$, $F_{PUSH Y}$ – longitudinal and transverse components of pushing force; R_X , R_Y – longitudinal and transverse components of the equivalent R; β_{PUSH} – drift angle of the tug hull, x_{PUSH} – point of pushing on ship.

Resulting force during pushing, therefore, can be described as an equilibrium of acting forces: reaction force of the ship; the hydrodynamic forces acting on the hull of the tug; the hydrodynamic forces acting on the thrusters; the hydrodynamic forces acting on the hull and thrusters resulting from their interaction.

$$F_{PUSH X} = R_X \cdot \cos\beta_{PUSH}; F_{PUSH Y} = R_Y \cdot \sin\beta_{PUSH} \quad (24)$$

$$F_{PUSH} = F_{PUSH X} + F_{PUSH Y} + F_{PUSH I} \quad (25)$$

where $F_{PUSH I}$ – towing interaction force.

Reacting forces can be described as follows:

$$\begin{aligned}
 X_{PUSH} &= F_{PUSH} \cdot \cos\beta_{PUSH} \\
 Y_{PUSH} &= F_{PUSH} \cdot \sin\beta_{PUSH} \\
 N_{PUSH} &= Y_{PUSH} \cdot x_{PUSH} \\
 K_{PUSH} &= Y_{PUSH} \cdot (z_{PUSH} - z_G)
 \end{aligned} \quad (26)$$

For the system, where several tugboats are involved in towing/pushing operations, the resultant force will take form:

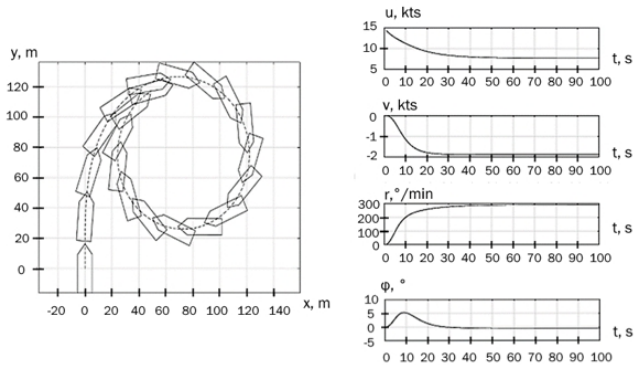
$$\begin{aligned}
 X_{PN} &= \sum_{n=1}^N X_{PULL n} + X_{PUSH n} \\
 Y_{PN} &= \sum_{n=1}^N Y_{PULL n} + Y_{PUSH n} \\
 N_{PN} &= \sum_{n=1}^N N_{PULL n} + N_{PUSH n} \\
 K_{PN} &= \sum_{n=1}^N K_{PULL n} + K_{PUSH n}
 \end{aligned} \quad (27)$$

where N – total number of tugs involved in pulling, n – tug number (from 1 to N).

4. Results of Simulation Modelling.

For the simulation purpose, Matlab Simulink R2016b modelling environment was used. Tug model selected for calculations has following characteristics: 50 t bollard pull; dimensions (L / B / d): 32.5 / 10.8 / 4.6 m; equipped with two azimuth thrusters, DP = 2.544 m. The result of the ASD tug model turning circle with both thrusters set to the angle of 35 degrees is shown in fig. 2 [23].

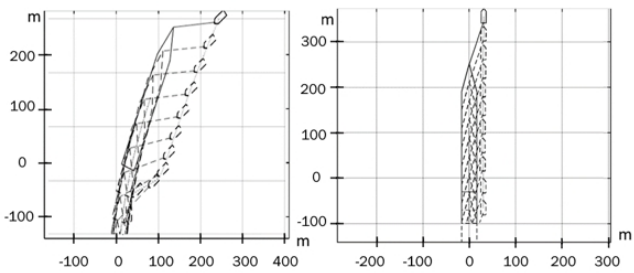
Figure 2: ASD tug starboard turn with thrusters? angle set to 35 degrees.



Source: Authors

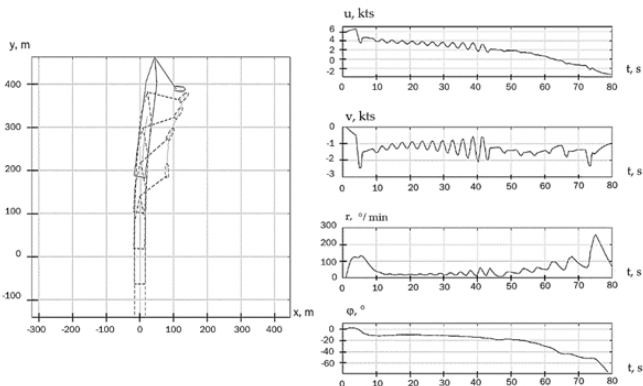
Mathematical model of a panamax-class container ship with dimensions (L / B / d): 282 / 32.2 / 12.2 m [23, 25], was used for the simulation of vessel-tug system dynamics (fig. 3, 4). In fig. 3 the simulation results of the different towing modes in the system “vessel-tug” are shown.

Figure 3: Vessel-tug system modelling: (a) mode bow-to-bow, speed 2 knots; (b) mode stern-to-bow, speed 4 knots.



Source: Authors

Figure 4: Vessel-tug system modelling - girting scenario; mode ?stern-to-bow?, speed 6 knots.



Source: Authors

The modelling of the “girting” scenario is shown in fig. 4, demonstrating a significant heeling of the tug - close to the

angle of vanishing stability and exceeds the angle of flooding (60°) for this type of tug. Such situation means capsizing, which in this experiment is caused by the moment formed between the forces of the thrust of the propeller and the tension on the towing line.

Based on the results of the study, the following critical features for the vessel-tug system operation may be emphasized from safe navigation perspective.

In “stern-to-bow” towing mode:

- synchronous steering mode with no limits may lead to a capsizing;
- both thrusters pushing against the towing line during girting may lead to capsizing;
- asynchronous steering mode with no limits may lead to large heeling angles;
- it is reasonable to keep one thruster for pushing and another for steering;
- at speed close to 8 knots thruster’s azimuths should be limited to a maximum of 40-50 degrees;
- tug heading has to be close (+/-10 degrees) to a towed vessel’s heading at speed not less than 4 knots;
- with higher speed, the higher heel is encountered by a tug. At 8 knots, in girting case, heel may exceed 40 degrees. At 4 knots with one thruster pushing sideways, heel may reach 15 degrees.

In “bow-to-bow” towing mode:

- at speed close to 8 knots thruster’s azimuths can be rotated up to 80 degrees in case the heading of the tug is equal to the vessel’s heading;
- tug’s heading should not exceed the difference in +/- 40 degrees compared to a towed vessel’s heading;
- with higher speed, the higher heel is encountered by a tug, when tug heading differs from the vessel heading.

Conclusions.

This paper considers the problem of the manoeuvring safety for vessel-tug system interaction. It is emphasized that the tug stability is rarely taken into account when planning and performing towing operations. Thus, in order to determine the critical operating modes, the mathematical model of the vessel-tug system which considers a flexible connection (tow wire) and allows the calculation of potentially hazardous towing modes is suggested. For the purpose of mathematical modelling an Azimuth Stern Drive tug and a Panamax container vessel were used. Simulation results allowed to formulate recommendations for “bow-to-bow” and “stern-to-bow” towing modes in order to prevent capsizing of the tug, which may be applied for planning and monitoring the vessel-tug system’s operations.

References.

1. Artyszuk J. 2014. Steady-state maneuvering of a generic ASD tug in escort pull and bow-rope aided push operation. Proceedings of TransNav, 8(3), pp. 449-457. DOI: 0.12716/1001.08.03.17

2. Bradner, P., Renilson, M. 1998. Interaction Between Two Closely Spaced Azimuthing Thrusters. *Journal of Ship Research*, 42(1), pp. 15-32.
3. Brandner, P. A. Performance and effectiveness of omnidirectional stern drive tugs: PhD Thesis. Tasmania, November 1995.
4. Dang, J., Laheij, H. 2004. Hydrodynamic Aspects of Steerable Thrusters. *Dynamic Positioning Conference*.
5. EMSA, 2021. Annual overview of marine casualties and incidents.
6. Ikeda, Y., Himeno, Y., Tanaka, N. 1978. A Prediction Method for Ship Rolling. Technical Report 00405. Department of Naval Architecture, University of Osaka Prefecture, Japan.
7. Hoffman, A.D. Propulsion-steering complex and vessel maneuvering. Handbook. Shipbuilding: Leningrad, USSR, 1988. 360 p.
8. Journée, J. M. J., Van Leeuwen, G. 2001. Prediction of Ship Maneuverability Making Use of Model Tests. Delft University of Technology. 65 p.
9. Kijima, K., Tanaka, S., Furukawa, Y., Hori, T. 1993. On a Prediction Method of Ship Manoeuvring Characteristics. *Proceedings of MARSIM-93*, 1, pp. 285–294.
10. Konon, N., Pipchenko O. 2021. Analysis of marine accidents involving container ships. *Shipping & Navigation (ISSN 2306-5761 | 2618-0073)*, 32, pp. 46-55. DOI:10.31653/2306-5761.32.2021.46-55
11. MAIB Accident report No 17/2008, September 2008. Report on the investigation of the loss of the tug Flying Phantom while towing Red Jasmine on the River Clyde.
12. MAIB Accident report No 10/2016, May 2017. Girting and capsize of mooring launch Asterix.
13. MAIB Accident report No 16/2017, July 2017. Capsizing of tug Domingue while assisting CMA CGM Simba resulting in two fatalities Tulear, Madagascar.
14. Mauro, F. 2021. Thrusters modelling for escort Tug capability predictions. *Ocean Engineering*, 229, 108967. <https://doi.org/10.1016/j.oceaneng.2021.108967>
15. Perez, T. 2005. A Review of Geometrical Aspects of Ship Motion in Maneuvering and Seakeeping, and the Use of a Consistent Notation. MSS Technical Report (MSS-TR001-2005), CeSOS, NTNU NO-7491, Trondheim, Norway, 30 p.
16. Perez T., Blanke, M. 2003. Mathematical Ship Modeling for Control Applications. (Technical Report). DTU Technical University of Denmark, 22 p.
17. Piaggio, B., Viviani, M., Martelli, M., & Figari, M. 2019. Z-Drive Escort Tug manoeuvrability model and simulation. *Ocean Engineering*, 191, 106461. <https://doi.org/10.1016/j.oceaneng.2019.106461>
18. Piaggio, B., Villa, D., & Viviani, M. 2020. Numerical analysis of escort tug manoeuvrability characteristics. *Applied Ocean Research*, 97, 102075. <https://doi.org/10.1016/j.apor.2020.102075>
19. Piaggio, B., Villa, D., Viviani, M., & Figari, M. 2020. Numerical analysis of escort tug manoeuvrability characteristics – Part II: The skeg effect. *Applied Ocean Research*, 100, 102199. <https://doi.org/10.1016/j.apor.2020.102199>
20. Piaggio, B., Viviani, M., Martelli, M., & Figari, M. 2021. Z-drive escort tug manoeuvrability modelling: From model-scale to full-scale validation. *Developments in Maritime Technology and Engineering*, 207–216. <https://doi.org/10.1201/9781003216599-23>
21. Piaggio, B., Viviani, M., Martelli, M., & Figari, M. 2022. Z-Drive Escort Tug manoeuvrability model and simulation, Part II: A full-scale validation. *Ocean Engineering*, 259, 111881. <https://doi.org/10.1016/j.oceaneng.2022.111881>
22. Pipchenko, O. D. 2017. Mathematical Modelling of Operation of The Tug Equipped With Azimuthal Thrusters. *Shipbuilding*, 2, pp. 13-19. DOI 10.15589/jnn20170202
23. Pipchenko, O.D. 2021. Development of theory and practice for the risk management of complex navigational tasks. D.Sc. Thesis. Odessa, 2021, pp. 161-169. Available online: www.onma.edu.ua/wp-content/uploads/2016/09/Dyssertatsyya-Pypchenko-pechat.pdf
24. Pipchenko, O.D., Tsymbal, M., Shevchenko, V. 2018. Recommendations for Training of Crews Working on Diesel-Electric Vessels Equipped with Azimuth Thrusters. *TransNav, the International Journal on Marine Navigation and Safety of Sea Transportation*, 12(3), pp. 567-571. DOI: 10.12716/1001.12.03.17
25. Pipchenko, O.D., Tsymbal, M., Shevchenko, V. 2020. Features of an Ultra-Large Container Ship Mathematical Model Adjustment Based on the Results of Sea Trials. *TransNav, the International Journal on Marine Navigation and Safety of Sea Transportation*, 14(1), pp. 163-170. DOI:10.12716/1001.14.01.20.
26. Quadvlieg, F., Kaul, S. 2006. Development of a calculation program for escort forces of stern drive tug boats. *International Tug & Salvage Convention & Exhibition, Rotterdam*.
27. The Shipowners' Mutual Protection and Indemnity Association (Luxembourg). Booklet – Loss Prevention. *Tug and Tows – A Practical Safety and Operational Guide 2015*.
28. Transportation Safety Board of Canada, Mode Transportation Safety Investigation Report M09W0141, 2009.
29. Transportation Safety Board of Canada, Mode Transportation Safety Investigation Report M18P0230, 2018.
30. Transportation Safety Board of Canada, Mode Transportation Safety Investigation Report M1P0246, 2020.
31. UNCTAD (2021). Review of Maritime Transport 2021 (United Nations publication. Sales No. E.21.II.D. 21. New York and Geneva. (2)
32. Voytkunsky, Y. I. Ship theory handbook: in 3 volumes. Editor: Voytkunsky, Y. I.; Shipbuilding: Leningrad, USSR, 1985. 544 p.

33. Yang, L., Lee, S.-S., & Sadakane, H. 2007. Influence of Ship-Tugboat Interaction on the Braking Performance of Tugboat Based on Model Experiments. *The Journal of Japan Institute of Navigation* 117(0), 135–142. <https://doi.org/10.9749/jin.117.135>
34. Yasukawa, H., Yoshimura, Y. 2015. Introduction of MMG standard method for ship maneuvering predictions. *Journal of Marine Science and Technology*, 10, pp. 37–52. DOI: 10.1007/s00773-014-0293-y
35. Yoshimura, Y., Masumoto, Y. 2012. Hydrodynamic database and manoeuvring prediction method with medium high-speed merchant ships and fishing vessels. *International MARSIM Conference*, pp. 494–503.